

Quark star matter in color-flavor-locked phase at finite temperature

Peng-Cheng Chu^{1,*} He Liu^{1,†} Min Ju^{2,‡} Xu-Hao Wu^{3,§} Hong-Ming Liu^{1,||} Ying Zhou^{4,¶}
Hao Liu,¹ Si-Yu Lu¹ and Xiao-Hua Li^{5,6,**}

¹*The Research Center for Theoretical Physics, Science School, Qingdao University of Technology, Qingdao, 266033, China*

²*College of Science, China University of Petroleum (East China), Qingdao, 266580, China*

³*School of Science, Yanshan University, Qinhuangdao 066004, China*

⁴*School of Physical Science and Technology, Inner Mongolia University, Hohhot, 010021, China*

⁵*School of Nuclear Science and Technology, University of South China, Hengyang, 421001, China*

⁶*Cooperative Innovation Center for Nuclear Fuel Cycle Technology and Equipment, University of South China, Hengyang, 421001, China*



(Received 7 June 2024; accepted 5 August 2024; published 23 August 2024)

We study the thermodynamic properties of the color-flavored-locked (CFL) quark matter in finite temperature and strong magnetic field cases within the confined-isospin-density-dependent-mass model. We find that considering the CFL phase in quark star (QS) matter can significantly influence the equation of state as well as the properties of QSs at finite temperature or under strong magnetic fields. In particular, our results indicate that the polytropic index becomes anisotropic under magnetic fields and decreases with the increment of the star mass at different isentropic stages of QSs.

DOI: [10.1103/PhysRevD.110.043032](https://doi.org/10.1103/PhysRevD.110.043032)

I. INTRODUCTION

One of the most challenging questions in nuclear physics and astrophysics is the exact composition of the compact stars, whose interior might be composed of deconfined strange quark matter (SQM) [1–4]. In Witten’s conjecture [5,6], SQM should be in the so-called “windows of stability” or satisfy the absolutely stable condition [the minimum energy per baryon at zero temperature may be less than $M(^{56}\text{Fe})/56 = 930$ MeV]. Then SQM might be considered as the true ground state of strongly interacting matter, which gives rise to a transition from nuclear matter to strange quark matter, and the neutron stars (NSs) or hybrid stars may be simultaneously converted to quark stars (QSs) once SQM appears in the inner core [7–9]. In many theoretical investigations, quark stars are figuring as the candidates of the substantial observed pulsars and cannot be totally ruled out [6,10–19]. Color-flavor-locked (CFL) quark matter, which would be the most symmetric pairing state [20–26], consists of the equal fractions of u , d , and s quarks at sufficiently high density and is calculated to be more stable than

SQM [27–31]. As predicted, CFL quark matter might exist inside the QSs or the inner core of the NSs [23,24], and studies have revealed that the equation of state (EOS) of CFL quark matter can support larger star mass than the EOS of SQM in QSs [25,32–34].

In theoretical research and the experiments from the heavy-ion collisions (HICs), the thermodynamical properties of dense strongly interacting matter can be obtained by investigating the QCD phase structure. In the meantime, people can also explore protoneutron stars (PNSs) after the type II supernova explosion to acquire the properties of the strongly interacting matter at finite temperature [35]. The transition from PNSs to protoquark stars (PQS) still lacks detailed understanding due to the complex burning process of hadron matter into SQM, and several works have been done to investigate the existence of PQS [15,36–42] without explaining how to produce them. For CFL quark matter, one can use isentropic stages along the star evolution line to calculate the properties of the star matter and quark stars in the CFL phase at finite temperature.

Compact stars can be endowed with extremely large magnetic fields, whose strength has been estimated about $B \sim 10^{14}$ at the star surface [43–45]. In the interiors of the magnetars, the magnetic field strength may increase to as large as $B \sim 10^{18}$ G [46] or even $B \sim 10^{20}$ G [47], which will break the spatial rotational $\mathcal{O}(3)$ symmetry and produce the anisotropic pressure of the star matter [47–50]. In order to describe the strength and the orientation distributions of the magnetic field inside the magnetars, people consider the

* Contact author: kyois@126.com

† Contact author: liuhe@qut.edu.cn

‡ Contact author: jumin@upc.edu.cn

§ Contact author: wuhaoyu@ysu.edu.cn

|| Contact author: liuhongming13@126.com

¶ Contact author: yingzhou@163.com

** Contact author: lixiaohuaphysics@126.com

density-dependent magnetic fields [51–56] and some extreme magnetic field orientation distributions [57,58], and the results indicate that both the strength and orientation distributions can significantly influence the properties of the star matter and magnetars under strong magnetic fields.

In the present work, we show that the exploration of Qs is of great importance to obtain the properties of the strongly interacting matter at finite temperature or under strong magnetic fields within the confined-isospin-density-dependent-mass (CIDDm) model. Through the consideration of the CFL quark phase, we investigate the thermodynamical properties of quark star matter and the maximum mass of Qs at finite temperature or under strong magnetic fields. We find that the CFL quark matter can indeed affect the EOS of quark matter in both finite temperature and strong magnetic field cases, and the star mass becomes larger by the stiffer EOS with the increasing nonvanishing pairing energy gap in the CFL quark phase. We also obtain that the polytropic index becomes anisotropic under magnetic fields and decreases with the increment of the star mass. This paper is organized as follows. In Sec. II, we derive the theoretical formalism of CFL quark matter at finite temperature or under strong magnetic fields within the CIDDm model. Then we present our calculation results about the properties of the quark star matter and quark stars in the CFL quark phase at finite temperature or under strong magnetic fields in Sec. III. Finally in Sec. IV, we provide our conclusion and discussion.

II. THE THEORETICAL FORMALISM

A. CFL matter at finite temperature

As shown in [5,6], SQM might be considered as the true ground state of QCD matter. In Ref. [34], the authors have shown that CFL quark matter is more stable than SQM quark matter within the CIDDm model at zero temperature, and the results also indicate that the maximum mass of Qs becomes larger in the CFL quark phase than that in SQM within CIDDm, which can satisfy most of the recent mass-radius constraint region of the pulsars from the experimental data. In the present work, we employ the CIDDm model to obtain the thermodynamical properties of the quark matter in the CFL phase at finite temperature and under strong magnetic fields. The detailed calculations of CIDDm model in SQM can be found in [57,59,60], where the CIDDm model is extended from the confined-density-dependent-mass (CDDm) model [61,62] to obtain stiffer EOSs with the isospin dependence being inside the equivalent quark mass. From large numbers of works on the EOS of quark star matter in the past decades, the EOS in general becomes stiffer by using density-dependent equivalent quark mass, increasing bag constant, or considering the repulsive interaction inside the quark matter [63–89] at zero temperature in order to support large mass pulsars.

In Ref. [60], the properties of SQM at finite temperature have been discussed by inserting the temperature dependence into the equivalent quark mass by considering the linear confinement and string tension $\sigma(T)$ [90,91], and the equivalent quark mass for CIDDm model at finite temperature is modified as

$$\begin{aligned} m_q &= m_{q_0} + m_I + m_{\text{iso}} \\ &= m_{q_0} + \frac{D}{n_B^z} - \tau_q \delta D_I n_B^\alpha e^{-\beta n_B}, \end{aligned} \quad (1)$$

with

$$\sigma(T) = 1 - \frac{8T}{\lambda T_c} \exp\left(-\lambda \frac{T_c}{T}\right), \quad (2)$$

where m_{q_0} is the current mass for each flavor of quarks (we set $m_{u0} = m_{d0} = 5.5$ and $m_{s0} = 80$ MeV in this work, which is identical with the current quark mass from Ref. [59]), $m_I = \frac{D}{n_B^z}$ is set as the density-dependent mass term with no isospin interaction, z is a quark mass scaling parameter to control the density dependence in m_I , and D is the parameter determined by considering the absolutely stable condition of SQM. The parameters D_I , α , and β in the isospin-dependent term m_{iso} are parameters determining the isospin dependence of the quark-quark effective interactions in quark matter. We also set $\tau_q = 1$ for $q = u$ (u quarks), $\tau_q = -1$ for $q = d$ (d quarks), and $\tau_q = 0$ for $q = s$ (s quarks) to show different isospin dependence among u , d , and s quarks, and the isospin asymmetry is defined as [59,83,92]

$$\delta = 3 \frac{n_d - n_u}{n_d + n_u}. \quad (3)$$

For the temperature-dependent term in the equivalent quark mass, $\sigma(T)$ is the temperature dependent string tension [93], $T_c = 170$ MeV is the critical temperature (which is calculated from LQCD [94], and this value is used in Refs. [90,91] for temperature dependence), and $\lambda = 1.605812$ is determined as the solution of the equation $1 - \frac{8T}{\lambda T_c} \exp(-\lambda \frac{T_c}{T}) = 0$ when $T = T_c$. Then one can obtain the quark confinement and asymptotic freedom by changing the baryon density n_B from zero to infinity in the equivalent quark mass within the CIDDm model.

The CFL quark phase, which is considered as the most symmetric pairing state, consists of paired quarks of all flavors and colors at sufficiently high baryon densities [21–23]. Quark matter in the CFL phase may appear in the interiors of the compact stars, exhibiting the identical fraction and chemical potential of u , d , and s quarks, which then excludes the leptons from the CFL quark matter due to the charge neutrality. From the results of Ref. [34], CFL quark matter is calculated to be more stable than SQM

at zero temperature within the CIDDMM model. For the finite temperature case of the quark star matter in the CFL quark phase, the density of each flavor of quarks can be written as

$$n_i = \frac{g_i}{2\pi^2} \int_0^\infty \left[\frac{1}{1 + e^{(\epsilon_i - \mu_i^*)/T}} - \frac{1}{1 + e^{(\epsilon_i + \mu_i^*)/T}} \right] p^2 dp + \frac{2\Delta^2 \mu_i^*}{\pi^2}, \quad (4)$$

where $g_i = 6$ is the value of the degeneracy factor for quarks, Δ is the nonvanishing pairing energy gap, ϵ_i means the energy spectrum of the i th flavor of quarks, and $\mu^* = \sum_i \mu_i^*/3$ is the effective term of the quark chemical potential μ_i . In CFL quark matter, the chemical potential of u , d , and s quarks satisfies $\mu_u = \mu_d = \mu_s$, and the detailed derivations of the effective term μ^* at finite temperature within the CIDDMM model can be found in Eqs. (16)–(18) from Ref. [75]. Then the thermodynamic potential density in the CFL phase at finite temperature can be written as

$$\Omega = -\sum_i \frac{g_i T}{2\pi^2} \int_0^\infty \left[\ln \left(1 + e^{-(\sqrt{p^2 + m_i^2} - \mu_i^*)/T} \right) + \ln \left(1 + e^{-(\sqrt{p^2 + m_i^2} + \mu_i^*)/T} \right) \right] p^2 dp - 3 \frac{\Delta^2 \mu^{*2}}{\pi^2}, \quad (5)$$

and the free energy density \mathcal{F} for CFL quark matter is expressed as

$$\mathcal{F} = \sum_i \mu_i n_i + \Omega. \quad (6)$$

The energy density at finite temperature can be obtained as $\mathcal{E} = \mathcal{F} + TS$, and S means the entropy density of the CFL quark phase which can be calculated as

$$S = -\sum_i \frac{\partial \Omega_i}{\partial T}. \quad (7)$$

B. CFL matter under strong magnetic fields

Since strong magnetic fields of magnetars might increase from $B = 10^{12} \rightarrow 10^{14}$ G on the surface [43–45] to $B = 10^{18} \rightarrow 10^{20}$ G in the core [46,47], we investigate the quark matter under strong magnetic fields in this subsection to obtain the thermodynamical properties of the star matter of magnetars in the magnetic CFL (MCFL) quark phase. According to [27–30,33], the authors calculate the properties of MCFL quark matter within the Nambu-Jona-Lasinio model and the quasiparticle model by considering the quark rotated charge procedure, and the thermodynamic potential density in the MCFL quark phase can be written as

$$\Omega_{\text{MCFL}} = \Omega_C + \Omega_N - 3 \frac{\Delta^2 \mu^{*2}}{\pi^2}, \quad (8)$$

where Ω_C and Ω_N are the contributions from the redefined charged and neutral quarks [27,30]. The charges of different colors of the quarks in the nine-dimensional flavor-color representation can be redefined as

$$\begin{array}{ccccccccc} \hline u_r & u_g & u_b & d_r & d_g & d_b & s_r & s_g & s_b \\ \hline 0 & 1 & 1 & -1 & 0 & 0 & -1 & 0 & 0 \\ \hline \end{array}. \quad (9)$$

Since the direction of magnetic field is assumed along the z axis [50–52], the contribution of the charged quarks Ω_C under magnetic fields in MCFL phase of the thermodynamical potential density within the CIDDMM model can be derived as

$$\Omega_C = -\sum_i \sum_{\nu=0}^{\nu_{\text{max}}^i} \frac{g_i (|q_i| B)}{2\pi^2} \alpha_\nu \left\{ \frac{1}{2} \mu_i^* \sqrt{\mu_i^{*2} - s_i(\nu, B)^2} - \frac{s_i(\nu, B)^2}{2} \ln \left(\frac{\mu_i^* + \sqrt{\mu_i^{*2} - s_i(\nu, B)^2}}{s_i(\nu, B)} \right) \right\}, \quad (10)$$

where $g_i = 2$ and $\alpha_\nu = 2 - \delta_{\nu,0}$. The expression of the contribution Ω_N from the neutral quarks is identical to the thermodynamic potential density of the CFL quark matter under zero magnetic field. Thus, μ_i^* in the MCFL phase within the CIDDMM model can be written as

$$\mu_i^* = \sqrt{k_{F,\nu}^2 + s_i(\nu, B)^2}, \quad (11)$$

where $s_i(\nu, B) = \sqrt{m_i^2 + 2\nu|q_i|B}$, and the upper Landau level ν_{max} is calculated as $\nu_{\text{max}}^i \equiv \text{int} \left[\frac{\mu_i^{*2} - m_i^2}{2|q_i|B} \right]$.

Then the expression of the chemical potential μ_i for charged u , d , and s quarks in MCFL quark matter under magnetic fields can be written as

$$\begin{aligned} \mu_i &= \frac{\sum_i \mu_i^* n_i}{\sum_i n_i} + \frac{1}{3} \sum_{j=u,d,s} \frac{3}{2\pi^2} \sum_{\nu=0}^{\nu_{\text{max}}^j} \alpha_\nu (|q_j| B) m_j \\ &\times \ln \left[\frac{k_{F,\nu}^j + \sqrt{k_{F,\nu}^j{}^2 + 2\nu|q_j|B + m_j^2}}{\sqrt{2\nu|q_j|B + m_j^2}} \right] \\ &\times \left\{ -\frac{zD}{n_B^{(1+z)}} - \tau_j D_I \delta [\alpha n_B^{\alpha-1} - \beta n_B^\alpha] e^{-\beta n_B} \right\}. \quad (12) \end{aligned}$$

In addition, the energy density $\mathcal{E}_{\text{MCFL}}$ of MCFL quark matter can be obtained by

$$\mathcal{E}_{\text{MCFL}} = \Omega_{\text{MCFL}} + \sum_i \mu_i n_i + \frac{B^2}{2}, \quad (13)$$

where $B^2/2$ comes from the contribution of the magnetic field. From [47,57], the $\mathcal{O}(3)$ rotational symmetry might be

broken, and then the pressure of the quark matter under strong magnetic field becomes anisotropic, which is defined as the longitudinal pressure P_{\parallel} being parallel to the magnetic field or the transverse pressure P_{\perp} being perpendicular to the magnetic field. In MCFL quark matter, the pressure of quark matter can also be anisotropic, and the expressions of the longitudinal pressure P_{\parallel} and the transverse pressure P_{\perp} are written as

$$P_{\parallel} = \sum_i \mu_i n_i - \mathcal{E}_{\text{MCFL}}, \quad (14)$$

and

$$P_{\perp} = \sum_i \mu_i n_i - \mathcal{E}_{\text{MCFL}} + B^2 - MB, \quad (15)$$

where $M = -\frac{\partial \Omega_c}{\partial B}$ is the system magnetization. One can further find that the longitudinal pressure P_{\parallel} can fulfill the Hugenholtz-Van Hove theorem, which guarantees the thermodynamical self-consistency in the MCFL quark phase within the CIDDMM model.

III. RESULTS AND DISCUSSIONS

A. Properties of CFL quark matter at finite temperature

In this work, we consider the parameter set as DI-85 ($D_I = 85 \text{ MeV} \cdot \text{fm}^{3\alpha}$, $D = 22.92 \text{ MeV} \cdot \text{fm}^{-3z}$, $z = 1.8$) within the CIDDMM model [59], which is capable of describing PSR J0348 + 0432 ($2.01 \pm 0.04 M_{\odot}$) as QSs in SQM under absolutely stable condition within CIDDMM model at zero temperature.

In Fig. 1, we show the free energy per baryon and pressure of SQM and CFL quark matter ($\Delta = 50$ and 100 MeV) as functions of baryon density at zero temperature and finite temperature cases ($T = 30$ and $T = 50 \text{ MeV}$). It can be seen that, from the left panel of Fig. 1, the minimum value of the free energy per baryon at zero temperature is less than 930 MeV (the minimum energy per baryon of the observed stable nuclei ^{56}Fe), satisfying the absolute stable condition of SQM. One can also find that the baryon density of the minimum free energy per baryon is exactly the corresponding zero pressure density from all of the cases in Fig. 1, which is consistent with the thermodynamical self-consistency and verifies the correctness of the derivation. Furthermore, we note that the free energy per baryon decreases with the increment of the temperature and the energy gap Δ in CFL quark phase, while the pressure increases with the temperature and Δ for both SQM and CFL quark matter. These findings suggest that the CFL quark matter might be more stable than SQM, and the EOS becomes stiffer when considering the CFL quark phase at larger Δ and T , which

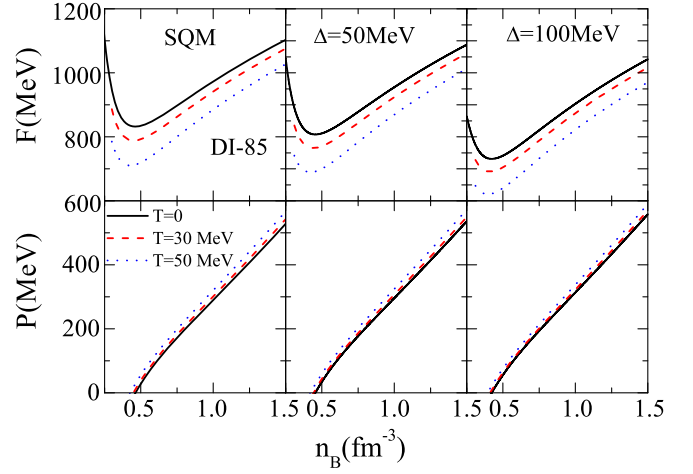


FIG. 1. Free energy per baryon and pressure as functions of baryon density at different temperature with DI-85 in SQM and the CFL phase with $\Delta = 50$ and 100 MeV .

implies that the CFL quark phase at finite temperature may provide a plausible description for heavier QSs.

Figure 2 shows the square of sound velocity ($c_s^2 = \partial P / \partial \epsilon$) as a function of the energy density at different temperatures in SQM and the CFL quark phase with $\Delta = 50$ and 100 MeV . One can find the sound velocity square decreases with the increment of the energy density and approaches the conformal matter case $c_s^2 = 1/3$ in the extremely large n_B region in all of the cases listed within the CIDDMM model. In addition, one can also see that the sound velocity increases with the temperature, which is consistent with the results in Fig. 1 that the EOS becomes stiffer as T increases. Moreover, it can be seen that c_s^2 decreases with Δ at the low energy density region (less than 600 MeV fm^{-3}) while increasing with Δ when the energy density is larger than 600 MeV fm^{-3} . For the results in Ref. [95], there exists

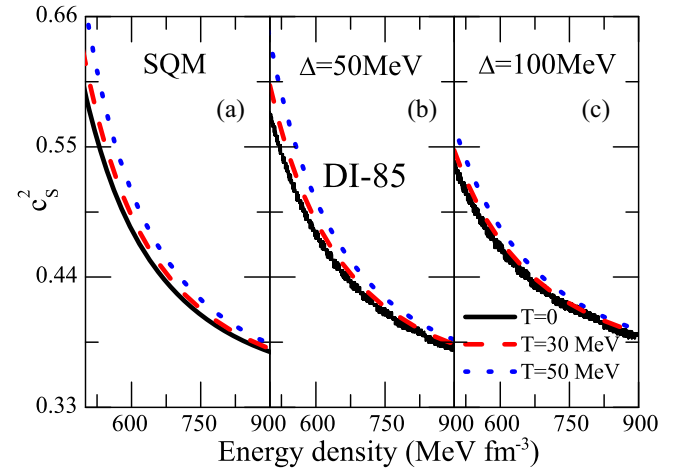


FIG. 2. Square of sound velocity as functions of energy density at different temperature with DI-85 in SQM and the CFL phase with $\Delta = 50$ and 100 MeV .

the peak of the sound velocity, which ensures the sound velocity satisfying the law of causality. From the results in Fig. 2, one can find the sound velocity increasing with the decrement of the energy density within the CIDDMM model. In our present work, the sound velocity is calculated by considering n_B being larger than the baryon density of the zero pressure point, and all listed results of the sound velocity square are calculated less than 1 for quark star matter, which satisfies the law of causality. Furthermore, the square of the sound velocity in Fig. 2 will decrease to approach the conformal limits $1/3$, and the convergence can also be found from the region $C_s^2 > 1/3$ in Fig. 5 from Ref. [96]. Following this, we calculate the polytropic index γ as functions of the baryon density in SQM and CFL quark phase at finite temperature in Fig. 3, whose expression is written as

$$\gamma = \frac{\partial \ln P}{\partial \ln \epsilon}. \quad (16)$$

One can find in Fig. 3 that the polytropic index γ decreases with the baryon density for both SQM and CFL quark matter cases in DI-85 within CIDDMM model, and γ also decreases with temperature at a fixed baryon density. Furthermore, the split of γ caused by considering the temperature effects decreases to zero in all of the cases when n_B becomes larger than 1 fm^{-3} , and the value of γ decreases from 1.22 to 1.12 from the SQM case to the $\Delta = 100 \text{ MeV}$ case at $n_B = 1 \text{ fm}^{-3}$, which is a bit larger than $\gamma = 1$ for the conformal boundary and fulfills the limit $\gamma < 1.75$ for pure quark matter from Ref. [97]. Moreover, we add the polytropic index line for the DI-3500 case ($D_I = 3500 \text{ MeV} \cdot \text{fm}^{3\alpha}$, $D = 13.81 \text{ MeV} \cdot \text{fm}^{-3z}$) within the CIDDMM model at zero temperature, and it is seen in

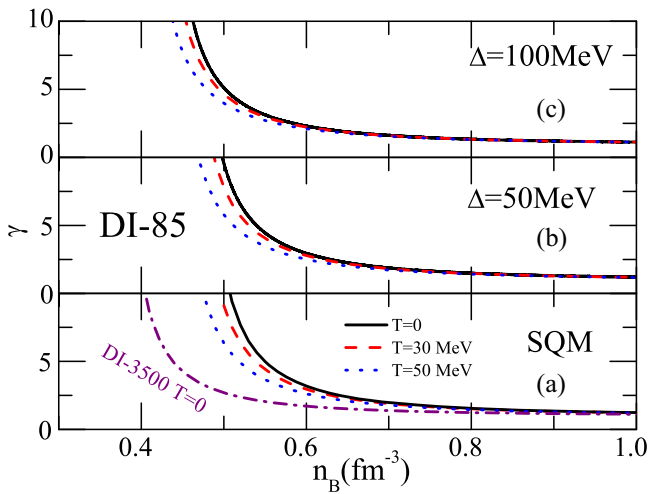


FIG. 3. The polytropic index as functions of the baryon density at different temperature with DI-85 in SQM and the CFL phase with $\Delta = 50$ and 100 MeV in panel (a), (b), and (c), respectively.

Fig. 3 that γ in the DI-3500 case is calculated much smaller than that in the DI-85 case. From [59], using the parameter set DI-3500 in SQM within the CIDDMM model can describe 2.38 solar mass QSs, which is the maximum star mass value the CIDDMM model can support (using DI-85 can only support 2.01 solar mass QSs). One can then conclude from Fig. 3 that γ decreases with the increment of the maximum star mass at zero temperature within the CIDDMM model.

In Fig. 4, we calculate the entropy per baryon as functions of n_B at $T = 30$ and $T = 50 \text{ MeV}$ in SQM and CFL quark matter with $\Delta = 50$ and 100 MeV . It is shown in Fig. 4 that the entropy per baryon decreases with n_B while increasing with the temperature. Furthermore, the entropy per baryon decreases with the energy gap Δ in the CFL quark phase at a certain temperature, implying that the degree of disorder for CFL quark matter can be reduced by considering a larger pairing energy gap.

As shown in Fig. 5, we calculate the mass-radius relation at different isentropic stages of quark stars with different Δ in the CFL quark phase with DI-85. One can find that the maximum star mass increases with the energy gap Δ at zero temperature in the CFL phase from the right panel. For the isentropic stages at finite temperature, the maximum star mass at $\Delta = 30 \text{ MeV}$ increases from $2.05M_\odot$ with $S/n_B = 1$ to $2.08M_\odot$ with $S/n_B = 2$, while the maximum star mass at $\Delta = 70 \text{ MeV}$ increases from $2.20M_\odot$ with $S/n_B = 1$ to $2.24M_\odot$ with $S/n_B = 2$, which indicates that the maximum star mass in the CFL quark phase at finite temperature increases with the entropy per baryon in the isentropic stages and the energy gap Δ . Moreover, we checked the central density of the maximum mass of QSs in the CFL quark phase, and we find the central density decreases from 1.2 to 1.18 fm^{-3} at the $S/n_B = 1$ stage while decreasing from 1.18 to 1.13 fm^{-3} at the $S/n_B = 2$ stage, when Δ

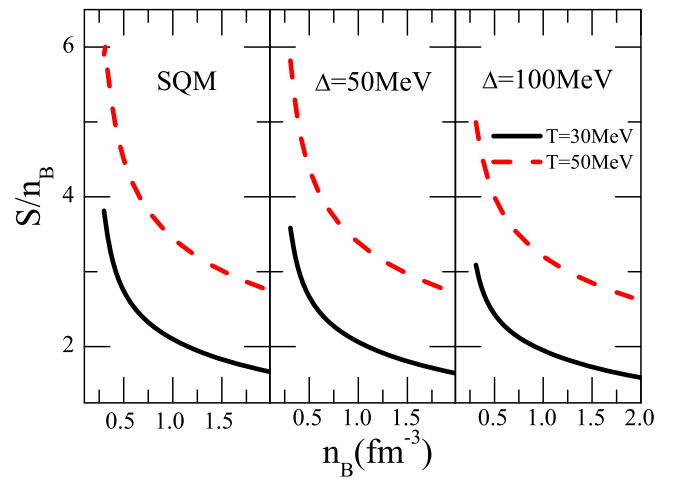


FIG. 4. Entropy per baryon as functions of the baryon density at different temperature with DI-85 in SQM and the CFL phase with $\Delta = 50$ and 100 MeV .

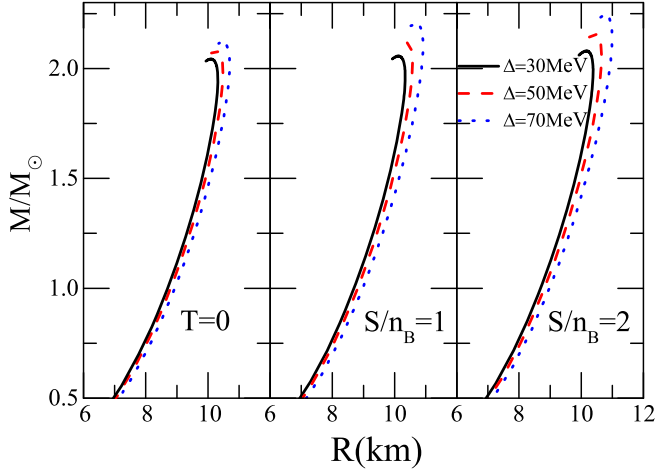


FIG. 5. Mass-radius relation at different isentropic stages of quark stars with different Δ .

increases from 30 to 70 MeV. This result implies that the central density of the maximum star mass in the CFL quark phase decreases with the maximum star mass.

In Fig. 6, we calculate the temperature of CFL quark matter as functions of the baryon density at different isentropic stages with different Δ . One can find from Fig. 6 that the temperature increases with the energy gap Δ for different isentropic stages, and the temperature at $S/n_B = 2$ stage is larger than that at the $S/n_B = 1$ stage at a certain n_B . Furthermore, we also calculate the core temperature T_C of the maximum star mass, and we note that T_C increases with Δ and the entropy per baryon. Then our results indicate that the entropy per baryon and the energy gap Δ can significantly influence the star mass and the temperature distribution inside the stars in the CFL quark phase within the CIDDM model.

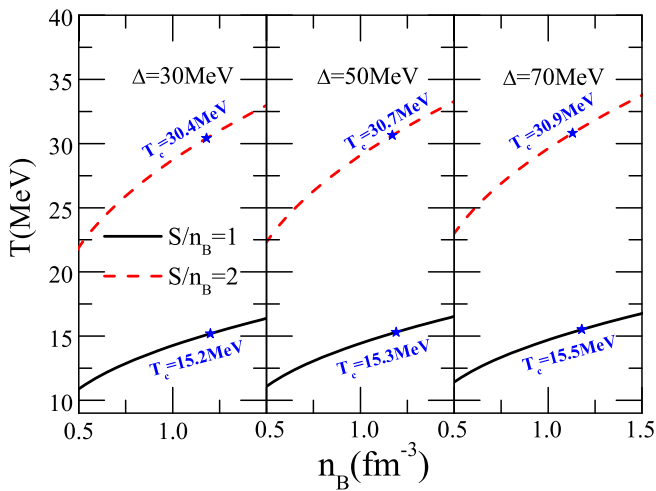


FIG. 6. Temperature of the quark star matter as functions of the baryon density at different isentropic stages with different Δ . The blue stars mark the core temperature T_c of the maximum star mass.

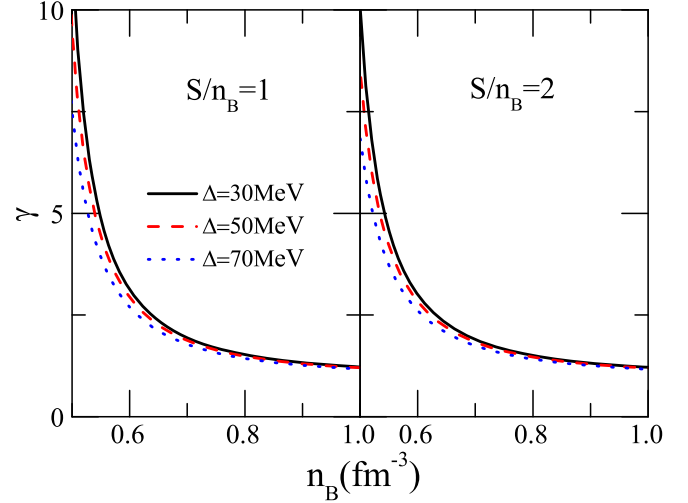


FIG. 7. The polytropic index as functions of the baryon density at different isentropic stages with DI-85 with different Δ .

In Fig. 7, we calculate the polytropic index as functions of the baryon density at different isentropic stages with different Δ . One can see from Fig. 7 that the polytropic index γ decreases with the baryon density in all cases, and γ also decreases with the energy gap Δ and the entropy per baryon. Since the maximum star mass from Fig. 5 increases with Δ and S/n_B , the results in Fig. 7 imply that the polytropic index γ of the star matter in CFL quark phase appears smaller in the heavier stars at isentropic stages within the CIDDM model.

B. Properties of quark matter and quark stars in MCFL phase

Figure 8 shows the energy per baryon and the anisotropic pressures as functions of the baryon density with DI-85 in SQM and CFL quark phase under magnetic fields. One can find that the minimum energy per baryon increases with the constant magnetic field B , which implies that the CFL quark matter becomes less stable once considering the magnetic field effects. The splitting between the longitudinal pressure P_{\parallel} and the transverse pressure P_{\perp} increases with the increasing strength of the magnetic field B , which can also be inferred from Eq. (15). One can also find that the zero pressure baryon density is exactly the baryon density of the minimum energy per baryon, which satisfies the thermodynamical self-consistency under strong magnetic fields.

Since the pressure becomes anisotropic under strong magnetic fields in MCFL quark matter, we calculate the anisotropic polytropic index in Fig. 9 as functions of the baryon density with DI-85 with different Δ under zero magnetic fields and strong magnetic fields ($B = 2 \times 10^{18}$ G). One can find in Fig. 9 that the polytropic index γ becomes anisotropic when considering the strong magnetic field, and then the anisotropic γ decreases with the baryon density in all cases. Furthermore, the values of γ

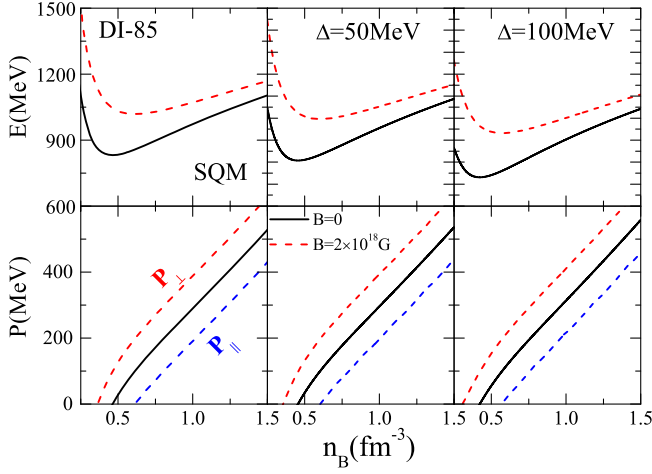


FIG. 8. Energy per baryon and anisotropic pressure as functions of the baryon density with DI-85 in SQM and the CFL quark phase under magnetic fields.

in the transverse pressure P_{\perp} case exhibit smaller values when the magnetic field increases to $B = 2 \times 10^{18}$ G, while the values of γ in the longitudinal pressure P_{\parallel} case become larger with magnetic field. It can also be seen in Fig. 9 that there appears an oscillatory behavior of γ with the baryon density increasing, and this oscillation is mainly caused by the upper Landau level in the energy density and the pressure of the quark matter under strong magnetic fields [the chemical potential for quarks in CFL quark phase (which is more stable than SQM) is less than that in SQM for a fixed baryon density, which will reduce the upper Landau levels].

In order to mimic the magnetic field strength inside the magnetars, we use the density-dependent magnetic field proposed by [51–56]

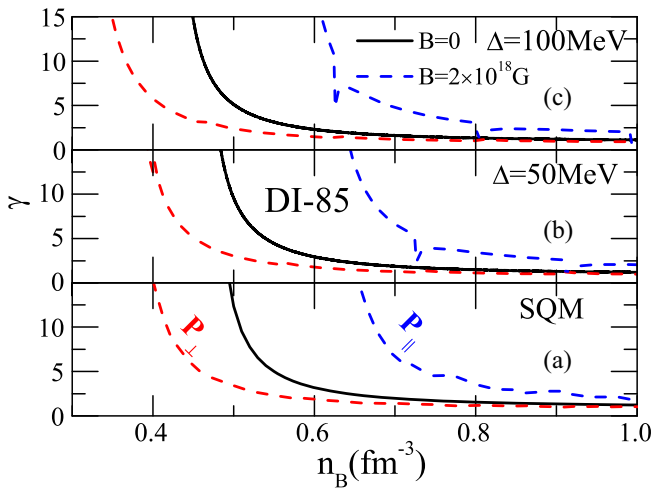


FIG. 9. The anisotropic polytropic index as functions of the baryon density with DI-85 under strong magnetic fields in SQM and the CFL phase with $\Delta = 50$ and 100 MeV in panel (a), (b), and (c), respectively.

$$B = B_{\text{surf}} + B_0[1 - \exp(-\beta_0(n_B/n_0)^\gamma)], \quad (17)$$

where the magnetic field of the star surface B_{surf} is set as 10^{15} G, n_0 is the saturation point of the nuclear matter, and B_0 is the vital parameter adjusting the real magnetic field inside the magnetars. In this work, we employ the fast-B profile from [57] to provide a strong density dependence of magnetic field strength from center to surface by considering $\gamma = 3$ and $\beta_0 = 0.001$. Furthermore, the orientation distributions of the magnetars we used in this work are denoted as “radial orientation” and “transverse orientation,” where the former means the local magnetic fields are along the radial direction while the latter using the magnetic fields perpendicular to the radial direction [57]. Then as shown in Fig. 10, we calculate the maximum mass of magnetars in the longitudinal and transverse orientation cases as functions of B_0 with $\Delta = 50$ and $\Delta = 70$ MeV. One can find the maximum mass of the magnetars increases/decreases with the increment of B_0 in the transverse/radial orientation case, which demonstrates an obvious star mass splitting caused by the magnetic orientation distribution. Furthermore, it can also be seen that the maximum star mass increases with Δ once the magnetic field is fixed. Since the polytropic index γ in the radial orientation case is larger than the γ in the transverse orientation case and γ decreases with the increasing Δ , the results imply that the polytropic index γ in CFL magnetar matter becomes smaller in the large star mass cases with large energy gap Δ or considering the transverse orientation distribution. In future works, the properties of the hot magnetized CFL quark matter should be discussed, which is of great importance to investigate the strongly interacting matter from the proto-magnetars and the experiments of the Large Hadron Collider. These works are in progress.

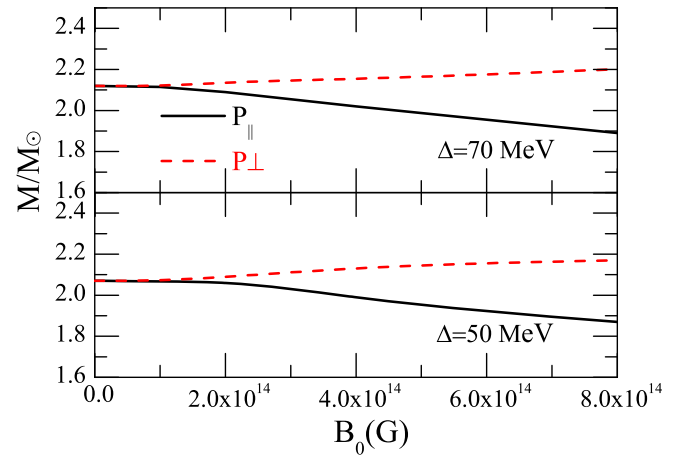


FIG. 10. The maximum mass of magnetars for the longitudinal and transverse orientation cases as functions of B_0 with different Δ .

IV. CONCLUSION AND DISCUSSION

In this work, we first investigate the free energy per baryon and the corresponding pressure of CFL quark matter. The results indicate that the free energy per baryon/pressure decreases/increases with the temperature and the pairing energy gap. Furthermore, we find the sound velocity square c_s^2 of the CFL quark matter is significantly influenced by Δ and increases with the temperature. We then calculate the polytropic index at finite temperature in the CFL quark phase, and the results indicate that γ decreases with Δ and T . We also find the entropy per baryon increases with T while decreasing with Δ .

Moreover, we calculate the mass-radius line at different isentropic stages. The results show that the maximum star mass and the core temperature increases with the entropy per baryon and the pairing energy gap, while the polytropic index decreases with the entropy per baryon and Δ , which also indicates that the polytropic index γ of the star matter in the CFL quark phase appears smaller in the heavier stars at isentropic stages within the CIDDMM model. We also calculate the polytropic index in the MCFL phase and the maximum star mass of the magnetars by considering both the density-dependent magnetic field and the two extreme

orientation distributions of the magnetic field inside the magnetars; the results indicate that both the polytropic index and the star mass of the magnetars become anisotropic under strong magnetic fields, which also implies that the polytropic index in CFL magnetar matter becomes smaller in the large star mass cases with large energy gap Δ or considering the transverse orientation distribution.

Therefore, our results indicate that considering CFL phase in quark star matter can significantly influence the equation of state as well as the properties of Qs at finite temperature or under magnetic fields, and the polytropic index becomes anisotropic under magnetic fields and decreases with the increment of the star mass at isentropic stages or under strong magnetic fields.

ACKNOWLEDGMENTS

This work is supported by the NSFC under Grants No. 11975132, No. 12205158, No. 12305148, and No. 11505100, and the Shandong Provincial Natural Science Foundation, China, No. ZR2022JQ04, No. ZR2021QA037, No. ZR2019YQ01, and No. ZR2015AQ007.

-
- [1] N. K. Glendenning, *Compact Stars*, 2nd ed. (Springer-Verlag Inc., New York, 2000).
 - [2] F. Weber, *Pulsars as Astrophysical Laboratories for Nuclear and Particle Physics* (IOP Publishing Ltd, London, 1999).
 - [3] J. M. Lattimer and M. Prakash, *Science* **304**, 536 (2004).
 - [4] A. W. Steiner, M. Prakash, J. M. Lattimer, and P. J. Ellis, *Phys. Rep.* **410**, 325 (2005).
 - [5] E. Witten, *Phys. Rev. D* **30**, 272 (1984).
 - [6] E. Farhi and R. L. Jaffe, *Phys. Rev. D* **30**, 2379 (1984).
 - [7] I. Bombaci, I. Parenti, and I. Vidana, *Astrophys. J.* **614**, 314 (2004).
 - [8] J. Staff, R. Ouyed, and M. Bagchi, *Astrophys. J.* **667**, 340 (2007).
 - [9] M. Herzog and F. K. Röpke, *Phys. Rev. D* **84**, 083002 (2011).
 - [10] A. R. Bodmer, *Phys. Rev. D* **4**, 1601 (1971).
 - [11] M. A. Stephanov, K. Rajagopal, and E. V. Shuryak, *Phys. Rev. Lett.* **81**, 4816 (1998).
 - [12] H. Terazawa, INS-Report No. 336, University of Tokyo, 1979.
 - [13] D. Ivanenko and D. F. Kurdgelaidze, *Lett. Nuovo Cimento* **2**, 13 (1969).
 - [14] N. Itoh, *Prog. Theor. Phys.* **44**, 291 (1970).
 - [15] C. Alcock, E. Farhi, and A. Olinto, *Astrophys. J.* **310**, 261 (1986).
 - [16] F. Weber, *Prog. Part. Nucl. Phys.* **54**, 193 (2005).
 - [17] P. C. Chu, Y.-Y. Jiang, H. Liu, Z. Zhang, X.-M. Zhang, and X.-H. Li, *Eur. Phys. J. C* **81**, 569 (2021).
 - [18] P. C. Chu, B. Wang, Y.-Y. Jia, Y.-M. Dong, S.-M. Wang, X.-H. Li, L. Zhang, X.-M. Zhang, and H.-Y. Ma, *Phys. Rev. D* **94**, 123014 (2016).
 - [19] P. C. Chu, X.-H. Li, B. Wang, Y.-M. Dong, Y.-Y. Jia, S.-M. Wang, and H.-Y. Ma, *Eur. Phys. J. C* **77**, 512 (2017).
 - [20] D. Bailin and A. Love, *Phys. Rep.* **107**, 325 (1984).
 - [21] M. G. Alford, K. Rajagopal, S. Reddy, and F. Wilczek, *Phys. Rev. D* **64**, 074017 (2001).
 - [22] I. A. Shovkovy, *Found. Phys.* **35**, 1309 (2005).
 - [23] K. Rajagopal and F. Wilczek, *Phys. Rev. Lett.* **86**, 3492 (2001).
 - [24] M. G. Alford, K. Rajagopal, T. Schaefer, and A. Schmitt, *Rev. Mod. Phys.* **80**, 1455 (2008).
 - [25] G. Lugones and J. E. Horvath, *Astron. Astrophys.* **403**, 173 (2003).
 - [26] J. E. Horvath and G. Lugones, *Astron. Astrophys.* **422**, L1 (2004).
 - [27] E. J. Ferrer and Vivian de la Incera, *Phys. Rev. Lett.* **95**, 152002 (2005).
 - [28] E. J. Ferrer, Vivian de la Incera, and Cristina Manuel, *Nucl. Phys.* **B747**, 88 (2006).
 - [29] B. Feng, E. J. Ferrer, and Vivian de la Incera, *Nucl. Phys.* **B853**, 213 (2011).
 - [30] L. Paulucci, Efrain J. Ferrer, Vivian de la Incera, and J. E. Horvath, *Phys. Rev. D* **83**, 043009 (2011).
 - [31] S. Sen, *Phys. Rev. D* **92**, 025004 (2015).
 - [32] G. Lugones and J. E. Horvath, *Phys. Rev. D* **66**, 074017 (2002).

- [33] P. C. Chu, Q. Cao, H. Liu, X.-H. Li, M. Ju, X.-H. Wu, and Y. Zhou, *Eur. Phys. J. C* **83**, 858 (2023).
- [34] P. C. Chu, H. Liu, X.-H. Li, M. Ju, X.-H. Wu, and X.-M. Zhang, *J. Phys. G* **51**, 065202 (2024).
- [35] M. Prakash, I. Bombaci, M. Prakash, P. J. Ellis, J. M. Lattimer, and R. Knorren, *Phys. Rep.* **280**, 1 (1997).
- [36] V. K. Gupta, Asha Gupta, S. Singh, and J. D. Anand, *Int. J. Mod. Phys. D* **12**, 583 (2003).
- [37] Jianyong Shen, Yun Zhang, Bin Wang, and Ru-Keng Su, *Int. J. Mod. Phys. A* **20**, 7547 (2005).
- [38] V. Dexheimer, J. R. Torres, and D. P. Menezes, *Eur. Phys. J. C* **73**, 2569 (2013).
- [39] V. Dexheimer, D. P. Menezes, and M. Strickland, *J. Phys. G* **41**, 015203 (2014).
- [40] A. Drago, A. Lavagno, and G. Pagliara, *Phys. Rev. D* **89**, 043014 (2014).
- [41] A. Drago and G. Pagliara, *Eur. Phys. J. A* **52**, 41 (2016).
- [42] A. Bauswein, N. Stergioulas, and H. Janka, *Eur. Phys. J. A* **52**, 56 (2016).
- [43] L. Woltjer, *Astrophys. J.* **140**, 1309 (1964).
- [44] T. A. Mihara, *Nature (London)* **346**, 250 (1990).
- [45] G. Chanmugam, *Annu. Rev. Astron. Astrophys.* **30**, 143 (1992).
- [46] D. Lai and S. L. Shapiro, *Astrophys. J.* **383**, 745 (1991).
- [47] E. J. Ferrer, V. Incera, Jr., P. Keith, I. Portillo, and P. L. Springsteen, *Phys. Rev. C* **82**, 065802 (2010).
- [48] A. A. Isayev and J. Yang, *Phys. Rev. C* **84**, 065802 (2011).
- [49] A. A. Isayev and J. Yang, *Phys. Lett. B* **707**, 163 (2012).
- [50] A. A. Isayev and J. Yang, *J. Phys. G* **40**, 035105 (2013).
- [51] D. Bandyopadhyay, S. Chakrabarty, and S. Pal, *Phys. Rev. Lett.* **79**, 2176 (1997).
- [52] D. Bandyopadhyay, S. Pal, and S. Chakrabarty, *J. Phys. G* **24**, 1647 (1998).
- [53] D. P. Menezes, M. Benghi Pinto, S. S. Avancini, A. Pérez Martínez, and C. Providência, *Phys. Rev. C* **79**, 035807 (2009).
- [54] D. P. Menezes, M. Pinto, Benghi, S. Avancini, and C. Providência, *Phys. Rev. C* **80**, 065805 (2009).
- [55] C. Y. Ryu, K. S. Kim, and Myung-Ki Cheoun, *Phys. Rev. C* **82**, 025804 (2010).
- [56] C. Y. Ryu, Myung-Ki Cheoun, T. Kajino, T. Maruyama, and Grant J. Mathews, *Astropart. Phys.* **38**, 25 (2012).
- [57] P. C. Chu, L. W. Chen, and X. Wang, *Phys. Rev. D* **90**, 063013 (2014).
- [58] D. Deb, B. Mukhopadhyay, and F. Weber, *Astrophys. J.* **922**, 149 (2021).
- [59] P. C. Chu and L. W. Chen, *Astrophys. J.* **780**, 135 (2014).
- [60] P. C. Chu and L. W. Chen, *Phys. Rev. D* **96**, 083019 (2017).
- [61] G. N. Fowler, S. Raha, and R. M. Weiner, *Z. Phys. C* **9**, 271 (1981).
- [62] G. X. Peng, H. C. Chiang, J. J. Yang, L. Li, and B. Liu, *Phys. Rev. C* **61**, 015201 (1999).
- [63] E. S. Fraga, R. D. Pisarski, and J. Schaffner-Bielich, *Phys. Rev. D* **63**, 121702(R) (2001).
- [64] E. S. Fraga and P. Romatschke, *Phys. Rev. D* **71**, 105014 (2005).
- [65] A. Kurkela, P. Romatschke, and A. Vuorinen, *Phys. Rev. D* **81**, 105021 (2010).
- [66] S. Chakrabarty, S. Raha, and B. Sinha, *Phys. Lett. B* **229**, 112 (1989).
- [67] S. Chakrabarty, *Phys. Rev. D* **43**, 627 (1991); **48**, 1409 (1993); **54**, 1306 (1996).
- [68] O. G. Benvenuto and G. Lugones, *Phys. Rev. D* **51**, 1989 (1995).
- [69] G. X. Peng, H. C. Chiang, B. S. Zou, P. Z. Ning, and S. J. Luo, *Phys. Rev. C* **62**, 025801 (2000).
- [70] G. X. Peng, A. Li, and U. Lombardo, *Phys. Rev. C* **77**, 065807 (2008).
- [71] A. Li, G. X. Peng, and J. F. Lu, *Res. Astron. Astrophys.* **11**, 482 (2011).
- [72] K. Schertler, C. Greiner, and M. H. Thoma, *Nucl. Phys. A* **616**, 659 (1997).
- [73] K. Schertler, C. Greiner, P. K. Sahu, and M. H. Thoma, *Nucl. Phys. A* **637**, 451 (1998).
- [74] P. C. Chu, X.-H. Li, H.-Y. Ma, B. Wang, Y.-M. Dong, and X.-M. Zhang, *Phys. Lett. B* **778**, 447 (2018).
- [75] P. C. Chu and L. W. Chen, *Phys. Rev. D* **96**, 103001 (2017).
- [76] P. C. Chu, X.-H. Li, H. Liu, M. Ju, and Y. Zhou, *Phys. Rev. C* **108**, 025808 (2023).
- [77] D. T. Son and M. A. Stephanov, *Phys. Rev. Lett.* **86**, 592 (2001).
- [78] M. Frank, M. Buballa, and M. Oertel, *Phys. Lett. B* **562**, 221 (2003).
- [79] D. Toublan and J. B. Kogut, *Phys. Lett. B* **564**, 212 (2003).
- [80] J. B. Kogut and D. K. Sinclair, *Phys. Rev. D* **70**, 094501 (2004).
- [81] L. He, M. Jin, and P. Zhuang, *Phys. Rev. D* **71**, 116001 (2005).
- [82] L. He and P. Zhuang, *Phys. Lett. B* **615**, 93 (2005).
- [83] M. Di Toro, A. Drago, T. Gaitanos, V. Greco, and A. Lavagno, *Nucl. Phys. A* **775**, 102 (2006).
- [84] G. Pagliara and J. Schaffner-Bielich, *Phys. Rev. D* **81**, 094024 (2010).
- [85] Z. Zhang *et al.*, *Phys. Rev. D* **103**, 023511 (2021).
- [86] G. Y. Shao, M. Colonna, and M. Di Toro, *Phys. Rev. D* **85**, 114017 (2012).
- [87] P. C. Chu, Y.-N. Wang, X.-H. Li, H. Liu, and J.-W. Zhang, *Phys. Rev. C* **105**, 045806 (2022).
- [88] H. Liu, J. Xu, and P.-C. Chu, *Phys. Rev. D* **105**, 043015 (2022).
- [89] Y. N. Wang, P.-C. Chu, Y.-Y. Jiang, X.-D. Pang, S.-B. Wang, and P.-X. Li, *Acta Phys. Sin.* **71**, 222101 (2022).
- [90] X. J. Wen, X. H. Zhong, G. X. Peng, P. N. Shen, and P. Z. Ning, *Phys. Rev. C* **72**, 015204 (2005).
- [91] Y. Zhang and R. K. Su, *Phys. Rev. C* **67**, 015202 (2003).
- [92] M. Di Toro, V. Baran, and M. Colonna, *J. Phys. G* **37**, 083101 (2010).
- [93] A. Ukawa, in *Proceedings of the 1993 Uehling Summer School: Phenomenology and Lattice QCD*, edited by G. Kilcup and S. Sharpe (World Scientific, Singapore, 1993), p. 231.
- [94] Zoltan Fodor and Sandor D. Katz, *J. High Energy Phys.* **03** (2002) 014.
- [95] Yuki Fujimoto, Kenji Fukushima, Larry D. McLerran, and Michal Praszalowicz, *Phys. Rev. Lett.* **129**, 252702 (2022).
- [96] Yuki Fujimoto and Kenji Fukushima, *Phys. Rev. D* **105**, 014025 (2022).
- [97] E. Annala, T. Gorda, A. Kurkela, J. Nättilä, and A. Vuorinen, *Nat. Phys.* **16**, 907 (2020).